Carbohydrate Polymers 121 (2015) 342–347

Contents lists available at ScienceDirect

Carbohydrate Polymers

journal homepage: www.elsevier.com/locate/carbpol

Effect of salt on turbulent drag reduction of xanthan gum

Cheng Hai Hong [a], Hyoung Jin Choi [a,*], Ke Zhang [b], Frederic Renou [c], Michel Grisel [c]

[a] Department of Polymer Science and Engineering, Inha University, Incheon 402-751, Republic of Korea
[b] School of Chemical Engineering and Technology, Harbin Institute of Technology, 150001 Harbin, People's Republic of China
[c] University of Le Havre, URCOM, EA 3221, FR CNRS 3038, 25 rue Philippe Lebon, B.P. 540, 76058 Le Havre Cedex, France

ARTICLE INFO

Article history:
Received 8 September 2014
Received in revised form
16 December 2014
Accepted 17 December 2014
Available online 5 January 2015

Keywords:
Xanthan gum
Turbulent drag reduction
Mechanical degradation

ABSTRACT

The turbulent flow of an aqueous KCl solution driven by a rotating disc in a closed chamber showed significant drag reduction (DR) when a small amount of xanthan gum (XG) was added. The effects of the experimental parameters (XG and KCl concentrations, and time) on the drag reduction efficiency were examined. While the DR efficiency of XG decreased with increasing salt (KCl) concentration, the time-dependent DR efficiency was found to be fitted well using Brostow model equation.

1. Introduction

The skin frictional drag of turbulent flow can be reduced remarkably using a small amount of additives through a process referred to the turbulent drag reduction (DR) (Benzi, 2010) in addition to non-additive passive DR systems (Abdulbari, Yunus, Abdurahman, & Charles, 2013). Among the various additives, polymeric additives have been predominant over others because significant DR performance can be expected even when the effective concentration of a polymer solution is very low. Polymer solution dynamics regarding the effects of polymer-induced turbulent drag reduction in very dilute solutions have become an important issue in both the scientific community (Malkin, Nesyn, Ilyusnikov, & Manzhai, 2001) and engineering fields (Burger, Chorn, & Perkins, 1980). Turbulent DR is defined as the drastic reduction of turbulent drag friction of a flowing medium using a small amount (ppm) of a suitable additive (Lim, Hong, Choi, Lai, & Chan, 2007). This suggests that such a flowing system requires a lower pressure gradient to maintain the same flow rate, in addition we can obtain a higher flow rate at a fixed pressure drop in a turbulent pipe flow. The DR in the turbulent flow of a dilute polymer solution was found to depend on a range of parameters, such as polymer concentration, temperature, type of polymer, etc. (Kim, Choi, Sung, Lee, & Jhon, 2005).

A range of long chain and flexible polymers are used in a drag reduction processing (Lim et al., 2007). Long and flexible polymer chains, such as poly(ethylene oxide) (Liberatore, Pollauf, & McHugh, 2003; Shetty & Solomon, 2009), poly(acryl amide) (Liberatore et al., 2003; Sung et al., 2004) and various biopolymers (Lim, Choi, & Chan, 2005; Abdulbari, Shabirin, & Abdurrahman, 2014) such as semi-flexible polysaccharide xanthan gum (Sohn et al. 2001; Wyatt, Gunther, & Liberatore, 2011; Kim, Choi, Kim, & Jhon, 1998; Amarouchene et al., 2008; Pereira, Andrade, & Soares, 2013) and guar gum (Kim, Lim, Choi, Sohn, & Jhon, 2002) have been studied widely as effective aqueous drag reducing agents (Pereira et al., 2013) in addition to polymer-surfactant systems (Mohsenipour & Pal, 2013; Suksamranchit, Sirivat, & Jamieson, 2006). On the other hand, the main problem of the mechanical degradation of polymers under strong turbulent flows still remains.

Xanthan gum (XG), a biopolymer with many interesting intrinsic physical characteristics, has been adopted in polymer dynamics and rheology as a model polymeric chain at both a molecular and a macroscopic level (Gilbert, Loisel, Savary, Grisel, & Picard, 2013; Gilbert, Picard, Savary, & Grisel, 2013; Renou, Petibon, Malhiac, & Grisel, 2013). As an anionic polysaccharide produced by a fermentation process from *Xanthomonas compestris*, its primary structure consists in repeated pentasaccharide units composed of 1-4-linked-β-D-glucose backbone substituted on every second unit with a charged trisaccharide side chain containing a D-glucuronic acid between two D-mannoses. The inner and terminal mannoses can be, respectively, substituted by an acetate and a pyruvate group. The degree of substitution of both acetate and pyruvate can vary according to the *X. campestris* strain used and fermentation conditions (Jansson, Kenne, & Lindberg, 1975). In an aqueous solution, it is well known that the XG adopts two different

* Corresponding author. Tel.: +82 32 860 7486; fax: +82 32 865 5178.
E-mail address: hjchoi@inha.ac.kr (H.J. Choi).

http://dx.doi.org/10.1016/j.carbpol.2014.12.015
0144-8617/

conformations: an ordered, rigid double-helix strand structure at low temperature and high ionic strength and a disordered, flexible coil state at high temperature and low ionic strength. This reversible order-to-disorder transition is characterized by a specific temperature named conformational temperature (T_m) (Christensen & Smidsrød, 1991; Morris, 1977; Norton, Goodall, Frangon, Morris, & Ress, 1984). Because the structure is highly extended in the solution, the molecules may align and associate via a hydrogen bonding to form a weakly structured material. Without added salt, backbone of the XG is disordered or partly ordered in the form of a randomly broken helix, but highly extended due to the electrostatic repulsions from the charged groups on the side chains. When the salt is added to the solution, a disorder–order transition occurs in which the backbone takes on a helical conformation, and the charged trisaccharide side chains collapse down onto the backbone and stabilize the ordered conformation. Thus the conformation of XG molecules can be tuned by adding salts such as NaCl or KCl (Braga, Azevedo, Marques, Menossi, & Cunha, 2006; Chun, Kim, & Lee, 2009; Camesano & Wilkinson, 2001; Muller, Anrhourrache, Lecourtier, & Chauveteau, 1986). Thereby, the XG has been widely used as a viscosity enhancing agent in different fields such as food, cosmetics, pharmaceutical industry and oil extraction.

On the other hand, the XG also has been widely used as a drag reducing agent, and its turbulent drag reduction behavior associated with a salt will be investigated in this study. Most studies of the drag reduction of XG/salt were performed using NaCl. The added salt ions interact with the anionic charges of the XG, inducing conformation changes of the XG in the solution, and then consequently resulting in a change in its shear viscosity. Note that the normalized zero shear rate viscosity for XG/KCl solution was observed to be higher than that of XG/NaCl solution attributed to the ionic radius of K ion which is much higher than that of Na ion (Wyatt & Liberatore, 2010). In contrast, XG/KCl was chosen in this study and the effect of XG on DR efficiency induced by KCl as a salt under turbulent flow was examined.

2. Experimental

A rotating disc apparatus (RDA) for the turbulent drag reduction experiment consisted of a stainless steel disc, 14.5 cm in diameter and 0.32 cm in thickness, which was enclosed in a cylindrical, temperature-controlled container composed of stainless steel, 16.3 cm in inner diameter and 5.5 cm in height, giving a volume of 370 ml. An electric transducer was used to monitor the torque on the disc rotating at 1980 rpm, yielding a specific Reynolds number, N_{Re} in this study.

In the case of external rotating disc flow, the turbulence can be observed at a rotational Reynolds number (N_{Re}) > 3×10^5, or equivalently, at a disc rotational speed (ω) > 570 rpm × 2π. Here, $N_{Re} \equiv \rho r^2 \omega/\mu$, where ρ is the fluid density, μ is the fluid viscosity and r is the radius of the disc. The temperature of the system was maintained at 25 ± 0.5 °C. The torque required to rotate the disc for a pure solvent (T_S) at a given speed was measured first. The percentage DR (%DR) was calculated by measuring the corresponding torque needed for a dilute polymer solution (T_P) at the same ω using the following equation (Pereira et al., 2013):

$$\%DR = \left[\frac{(T_s - T_p)}{T_s}\right] \times 100 \quad (\text{at a given } N_{Re} \text{ number}) \qquad (1)$$

Both XG and KCl were purchased from Sigma Chemical Co. The RDA reservoir was filled with a solution volume of 370 ml containing 10, 50, 100 and 200 ppm XG with different concentrations of KCl (0 M, 0.01 M and 0.1 M), respectively. First, a 5% stock solution of XG/KCl was prepared. The %DR was then obtained as a function of time by injecting the measured quantities of stock solution directly into the turbulent flow field generated by RDA.

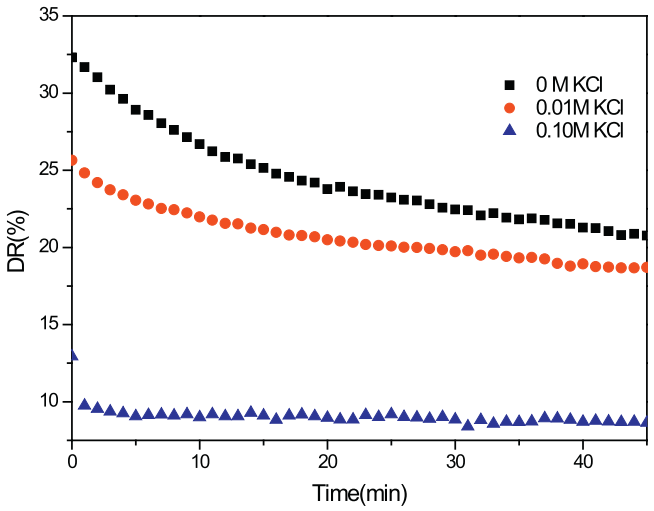

Fig. 1. Drag reduction efficacy as a function of various concentrations of KCl for 50 ppm XG.

The rheological properties of the XG/KCl solutions (10, 50, 100, and 200 ppm XG without KCl at 0, 0.01, and 0.1 M KCl for 200 ppm XG) were examined using a rotational rheometer (Physica MC300, Stuttgart, Germany) equipped with a Couette flow geometry (DG25) at 25 °C. The steady shear viscosity was measured as a function of shear rate in the range of 0.1 to 1000 s^{-1} in a controlled shear rate mode.

Proton NMR was used to determine pyruvate and acetate contents. Five milligrams of xanthan were dissolved in 1 ml of water in the presence of sodium acetate (5×10^{-3} M) as internal standard. The samples were lyophilized and then re-dissolved in D2O. Proton spectra were recorded at 300 MHz on a Bruker Avance 300 spectrometer; they were obtained at 80 °C and 128 scans were performed. Two peaks at 1.5 and 2.1 ppm were attributed to pyruvate and acetate groups (Rinaudo, Milas, & Lambert, 1983). Quantitative contents of acetate and pyruvate groups were calculated from the integrals of ^{1}H signals, in comparison to sodium acetate.

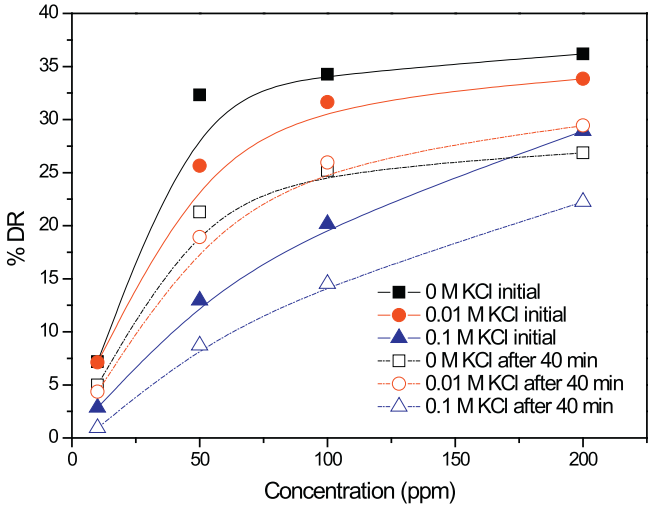

Fig. 2. Concentration dependence of %DR with XG.

3. Results and discussion

To examine the salt effect on the drag reduction efficacy with XG, the %DR was observed for salt solutions at three different concentrations (0, 0.01 and 0.1 M KCl) with a rotational speed of 1980 rpm at 25 °C as a function of the operating time, as shown in Fig. 1 with 50 ppm XG. The %DR decrease was quite apparent with increasing salt concentration. The resisting and residual drag reducing efficiency is believed to have originated from the residual cut XG in turbulent flow. With 0, 0.01 and 0.1 M KCl, the XG showed 32%, 26% and 13% of a drag reducing efficiency of initial %DR, respectively. Fig. 1 also showed a decreased drag reducing efficiency of 21%, 7% and 4%, respectively, at 40 min, explaining that the drag reduction efficacy for a salt concentration of 0 and 0.01 M decreased rapidly compared to that of higher concentration in the measurement time range of 20 min. From a view point of mechanical strength of XR chains in the solution, the drag reduction efficacy for a salt concentration of 0.1 M was relatively stable over time, suggesting that the mechanical degradation of the XG becomes less severe for a higher salt concentration.

To observe concentration effect on drag reduction of the XG more clearly, the %DR was measured as a function of the xanthan concentration at 1980 pm, as shown in Fig. 2. As a general trend, one can observe an increase in %DR with increasing XG concentration. On the other hand, the evolutions of %DR with salt concentration and time are more complicated and will be developed the next section. The %DR efficiencies of the XG/KCl became lower in higher concentrations of KCl. It could be related to the fact that polymer chain conformation of the XG becomes more rigid, resulting in less sensitivity to the high shear condition.

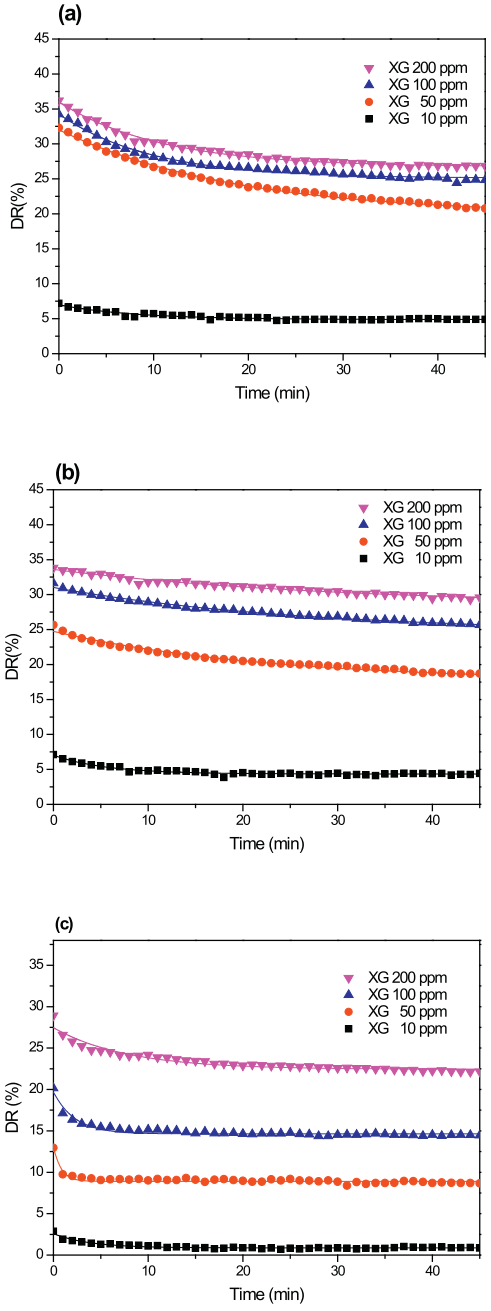

Fig. 3. Plots of %DR of XG with (a) 0 M, (b) 0.01 M, and (c) 0.1 M KCl for different concentration of XG: the data are fitted with lines of Eq. (2).

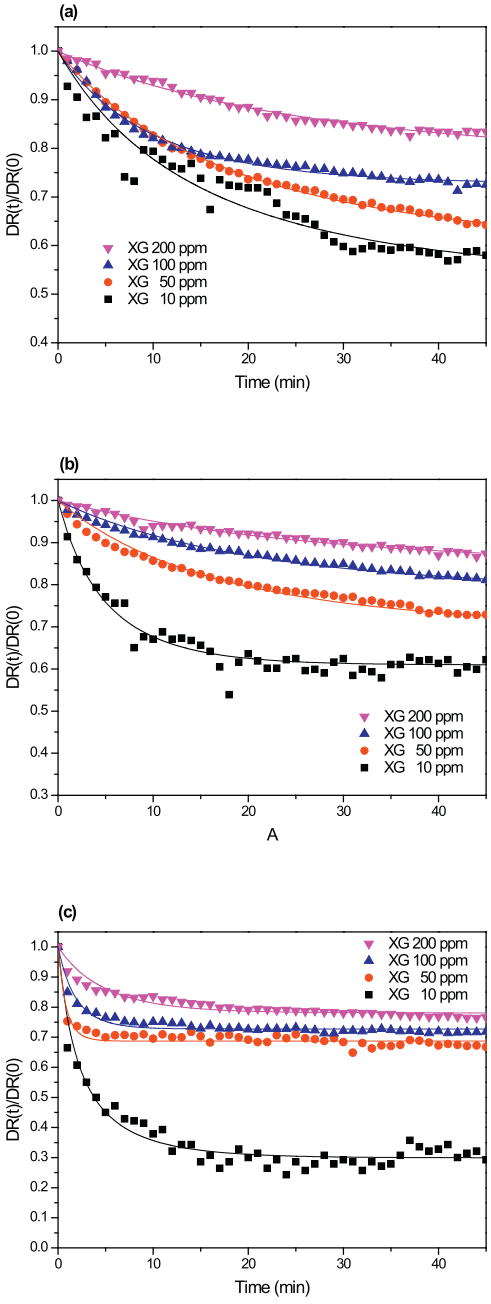

Fig. 4. Plots of %DR of XG with (a) 0 M, (b) 0.01 M, and (c) 0.1 M KCl for different concentration of XG: the data are fitted with lines of Eq. (3).

A previous study investigated the relationship between the molecular weight of the polymer and drag reduction (Choi, Lim, Lai, & Chan, 2002). The drag reduction efficiency was fitted using the following equation:

$$\%\mathrm{DR}(t) = w(L)N_L(t) + w\left(\frac{L}{2}\right)N_{L/2}(t) + c = w_1 e^{-at} + 2w_2\left(1 - e^{-at}\right) + c \quad (2)$$

where $w(L)$ is the drag reducing power dependence, $N_L(t)$ and $N_{L/2}(t)$ are the number of polymer with length L and $L/2$ at time t, respectively, and w_1, w_2, and c are the fitting parameters. The rate constant "a" with the unit of a reciprocal time (1/s) contains information on the dynamics of mechanical degradation of the polymer chain. Because the XG samples are not mono-dispersed, it is difficult to determine if the chain of XG dissociates into two chains with the same length. On the other hand, Eq. (2) was applied for XG, assuming that the most probable area of chain scission would be in the middle.

Fig. 3 shows the decay of the drag reduction efficiency as a function of time, and the symbols represent experimental data obtained and the lines are given by Eq. (2). Table 1 shows the parameters for the fitted lines in Fig. 3. The tendency of exponential decay with Eq. (2) showed good agreement with the data except for the initial 10 min. With increasing XG concentration, the a parameter generally decreased and w_1, w_2, and c increased. The value of w_1 is found to be larger than w_2, supporting that w_1's contribution to the %DR is more significant than w_2. That is, a higher XG concentration initially leads to more effective work of XG on drag reduction, and the drag reduction efficiency decays slowly, even though turbulence with higher energy is expected to cut the chains more severely. From Table 1, it can be observed that with the increase of KCl concentration, w_1 value decreased, which may indicate that the chain length becomes shorter, leading to the lower %DR value. However, one should keep in mind that when KCl concentration increased, the xanthan molecules were compacified due to the disorder to order transition, thus leading to a more compact conformation. So the apparent decrease in w_1 is more related to change in xanthan conformation than to chain length reduction.

Another model to describe the deteriorating drag reduction efficiency has been suggested (Brostow, 2008) as in the following equation:

$$\frac{\mathrm{DR}(t)}{\mathrm{DR}(0)} = \frac{1}{\left[1 + W\left(1 - e^{-ht}\right)\right]} \quad (3)$$

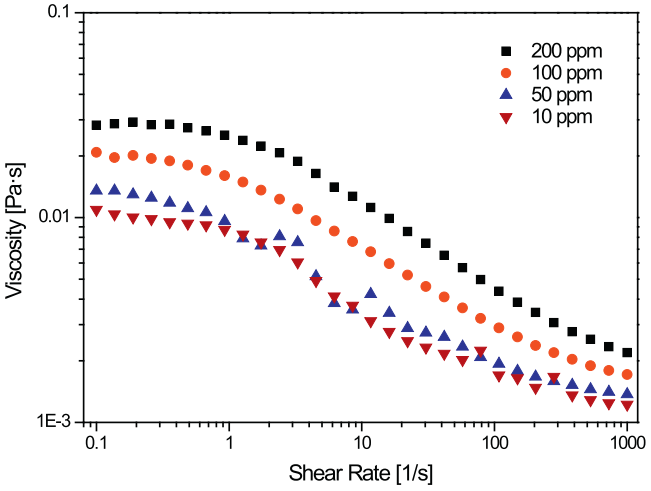

Fig. 5. Shear viscosity as a function of various concentrations of XG without salt.

where the parameter W is related to the shear stability, and parameter h is related to the degradation rate. A large h value indicates rapid degradation, whereas a larger W value implies low shear stability. In addition, more terms for h were suggested, which is now a function of the polymer concentration. On the other hand, Eq. (3) was preferred in this study. Table 1 also lists the parameters of Eq. (3) for various conditions. The comprehensive tendency for concentration was difficult to determine. Fig. 4 shows the drag reduction efficiency (DR(t)/DR(0)) fitted using Eq. (3) for a series of XG/KCl solutions at 25 °C. The curve showed a good fit under all conditions for XG/KCl solutions. The decreased value of W with increasing concentration of XG means that the shear stability was reduced with increasing concentration of XG. In addition, W also decreased with an increase of the XG concentration for all KCl concentrations. However, the value of W fluctuated with increasing concentration of KCl. However, the value of h does not always decrease with increasing concentration of XG, while the %DR increases with increasing concentration of XG. This might be related to the fluctuation of the data for its fitting as can be seen from the regression coefficient (chi-squared) given in Table 1.

The rheological properties of XG/KCl solutions can provide information on the molecular conformation. Figs. 5 and 6, respectively, show the shear viscosity as a function of the XG concentration without added salt and as a function of KCl concentration for 200 ppm XG. For the XG/KCl solution, the viscosity increased with increasing

Table 1
Parameters for the fitted lines of Eqs. (2) and (3).

	KCl (M)	Eq. (2)							Eq. (3)		
		a (1/s)		w_1	w_2	c	Reduced Chi-Sqr	Adj. R-square	W	h	Adj. R-square
		Value	Std								
XG 10 ppm	0	0.124	0.0123	2.978	0.435	4.012	0.0251	0.9206	0.876	0.039	0.9248
	0.01	0.178	0.0128	3.143	0.232	3.885	0.0231	0.9359	0.641	0.137	0.9356
	0.1	2.583	0.0210	0.209	0.751	2.368	0.0099	0.9175	2.341	0.147	0.9369
XG 50 ppm	0	0.054	0.0019	20.689	4.274	11.339	0.0555	0.9947	0.691	0.035	0.9968
	0.01	0.044	0.0024	14.872	3.868	9.879	0.0516	0.9854	0.437	0.044	0.9787
	0.1	1.242	0.0180	7.281	1.644	5.617	0.0540	0.8557	0.455	0.981	0.8660
XG 100 ppm	0	0.103	0.0043	21.414	6.122	2.846	0.0789	0.9867	0.376	0.080	0.9897
	0.01	0.038	0.0017	18.378	5.941	12.651	0.0226	0.9918	0.276	0.040	0.9853
	0.1	0.442	0.0365	11.519	3.245	8.140	0.0621	0.9225	0.375	0.422	0.9351
XG 200 ppm	0	0.093	0.0030	22.463	6.594	13.531	0.0466	0.9925	0.284	0.031	0.9872
	0.01	0.033	0.0025	19.495	7.146	14.106	0.0293	0.9822	0.187	0.032	0.9811
	0.1	0.128	0.0119	16.126	5.557	11.324	0.1252	0.9277	0.281	0.170	0.9045

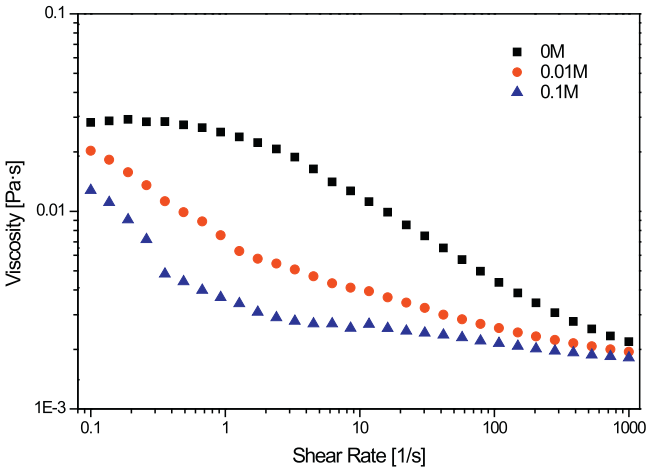

Fig. 6. Shear viscosity as a function of various concentrations of KCl for 200 ppm.

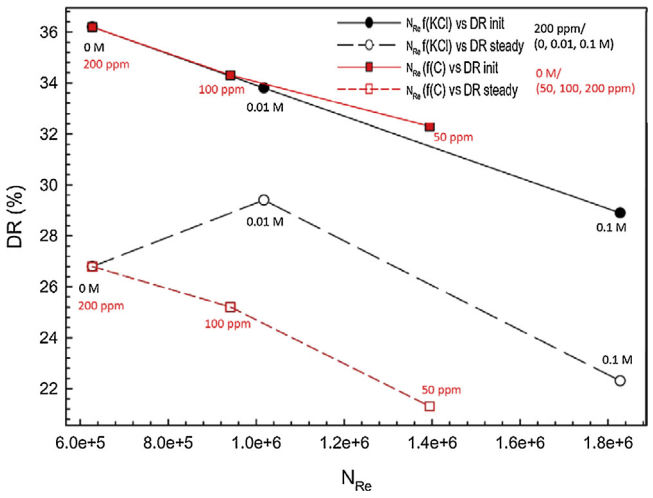

Fig. 7. Some calculation of N_{Re} and plotted initial and after 40 min %DR vs N_{Re} for C_{XG} = 200 ppm at different KCl concentrations and KCl = 0 at different XG concentrations.

XG concentration, and decreasing KCl concentration for 200 ppm XG, regardless of the XG and salt concentrations.

Such behavior with salt solutions was explained by the salt-induced, disorder–order transition, and the tendency to strengthen the intermolecular associations between the xanthan molecules. The viscosity increased with decreasing ionic strength within this low xanthan concentration regime, and a more complex dependence on the concentration was observed. The addition of salt promotes the screening of electrostatic repulsion of the trisaccharide side chains, allowing for the adoption of a much more compact helical backbone conformation (Braga et al., 2006) which implies a lower hydrodynamic volume and thus a lower viscosity within the dilute regime.

Therefore, the shear viscosity of XG is a function of the type of salt and its concentration (Morris, 1977; Norton et al., 1984; Muller et al., 1986). Obviously, as the ionic strength increased, i.e. salt concentration increased, the shear viscosity decreased below the entangled XG solutions (Wyatt & Liberatore, 2010). The shear viscosity of the XG solutions without salt addition was higher than those with salt addition (Tam & Tiu, 1993). In a XG/KCl solution, the electronic repulsions between like-charges along the XG backbone stretch and elongate individual chains. The counter ions surround the XG chains to balance the charge on the XG chain and maintain charge neutrality of the solution. With the electrostatic interactions, the extended configuration of the XG chains, accounts for some of the interesting rheological properties of XG solutions. In XG/KCl solution, the addition of counter ions allows the chain of XG to order and assume a smaller, more compact structure. The degree to which a molecule compacifies depends on the rigidity of the XG chain in the solution. As the molecular configuration changes, the solution rheology follows. In the XG/KCl solutions, the compact polymer chains lead to a reduction in shear viscosity. However, the shear thinning behavior of the XG solutions with salt exhibits complex phenomenon of the slope changes as shown in Fig. 6 (Lee & Brant, 2002) which might be also related to the complex confirmation change of the XG in a solution with either anisotropic or isotropic in addition to different states of an ordered, helical and a disordered conformation depending on the solution ionic strength (Wyatt and Liberatore, 2010). In addition, from $N_{Re} \equiv \rho r^2 \omega/\mu$, Reynolds number is inversely proportional to the viscosity. As we know, %DR increases with a turbulent strength, i.e., Reynolds numbers (Kim, Jo, Choi, Kim, & Jhon, 2001). Thus, a decrease in viscosity for XG solutions with KCl addition will cause an increase in the %DR of XG/KCl solutions. The effect of salt can increase the rigidity of polymer, therefore, they can affect the drag, the flow, and %DR (Amarouchene et al., 2008). Eventually results in the decrease of salt concentration increased %DR effect. It can be also noted that such a shear thinning behavior has been also observed for both a commercial non-aqueous drag reducer and polyisobutylene in kerosene (Tiu, Moussa, & Carreau, 1995).

According to our calculation of N_{Re} and plotted %DR (initial and after 40 min) vs N_{Re} for 200 ppm XG at different KCl concentrations and without KCl at different concentration of XG (see Fig. 7), we can observe two different things: first, the initial %DR just depends linearly on the N_{Re} whatever if XG is disordered or ordered thus nor XG conformation or concentration do not play a role on initial %DR, just the viscosity counts. Second, after 40 min, XG without salt, i.e. disordered, is much more affected by high shear then once XG ordered, %DR follow the same tendency than the initial %DR (only values are lower). This means contrary to what is observed for the initial %DR, ordered XG is much less sensitive to "fatigue" due to its rigid conformation. The acetate and pyruvate contents of XG were measured by NMR, which revealed 79% acetate and 43% pyruvate. The XG branching structure and its rigid conformation explains its higher rheological characteristics better than most of the other commonly available polysaccharides. On the other hand, it should be noted that Fig. 7 does not represent the general trend of %DR as a function of N_{Re} in a rotating disk apparatus as observed previously, in which the %DR increases with N_{Re} for a fixed polymer solution but only increasing the rotation speed (Kim et al., 2001).

4. Conclusion

This study examined the turbulent drag reduction efficiency induced by XG in KCl solutions with different concentrations. The chain degradation behavior with time decreased at higher KCl concentrations. In addition, the turbulent drag reduction efficiency induced by XG at different concentrations was analyzed. The drag reduction was enhanced at higher XG concentrations. Although both the Brostow and the models proposed in this study could describe the drag reduction behavior in turbulent flow, the Brostow model was found to better fit the experimental data under all conditions.

Acknowledgment

This study was supported by research grants of 39704-1 from National Research Foundation of Korea (2009).

References

Abdulbari, H. A., Yunus, R. M., Abdurahman, N. H., & Charles, A. (2013). Going against the flow—A review of non-additive means of drag reduction. *Journal of Industrial and Engineering Chemistry*, *19*, 27–36.

Abdulbari, H. A., Shabirin, A., & Abdurrahman, H. N. (2014). Bio-polymers for improving liquid flow in pipelines—A review and future work opportunities. *Journal of Industrial and Engineering Chemistry*, *20*, 1157–1170.

Amarouchene, Y., Bonn, D., Kellay, H., Lo, T. S., L'Vov, V. S., & Procaccia, I. (2008). Reynolds number dependence of drag reduction by rodlike polymers. *Physics of Fluids*, *20*. Art No. 065108.

Benzi, R. (2010). A short review on drag reduction by polymers in wall bounded turbulence. *Physica D: Nonlinear Phenomena*, *239*, 1338–1345.

Braga, A. L. M., Azevedo, A., Marques, M. J., Menossi, M., & Cunha, R. L. (2006). Interactions between soy protein isolate and xanthan in heat-induced gels: The effect of salt addition. *Food Hydrocolloids*, *20*, 1178–1189.

Brostow, W. (2008). Drag reduction in flow: Review of applications, mechanism and prediction. *Journal of Industrial and Engineering Chemistry*, *14*, 409–416.

Burger, E. D., Chorn, L. G., & Perkins, T. K. (1980). Studies of drag reduction conducted over a broad range of pipeline conditions when flowing prudhoe bay crude oil. *Journal of Rheology*, *24*, 603–626.

Camesano, T. A., & Wilkinson, K. J. (2001). Single molecule study of xanthan conformation using atomic force microscopy. *Biomacromolecules*, *2*, 1184–1191.

Choi, H. J., Lim, S. T., Lai, P. Y., & Chan, C. K. (2002). Turbulent drag reduction and degradation of DNA. *Physical Review Letters*, *89*. Art No. 088302.

Christensen, B. E., & Smidsrød, O. (1991). Hydrolysis of xanthan in dilute acid: Effects on chemical composition, conformation, and intrinsic viscosity. *Carbohydrate Research*, *214*, 55–69.

Chun, M. S., Kim, C., & Lee, D. E. (2009). Conformation and translational diffusion of a xanthan polyelectrolyte chain: Brownian dynamics simulation and single molecule tracking. *Physical Review E: Statistical, Nonlinear, and Soft Matter Physics*, *79*. Art No. 051919.

Jansson, P.-e., Kenne, L., & Lindberg, B. (1975). Structure of the extracellular polysaccharide from xanthomonas campestris. *Carbohydrate Research*, *45*, 275–282.

Gilbert, L., Loisel, V., Savary, G., Grisel, M., & Picard, C. (2013). Stretching properties of xanthan, carob, modified guar and celluloses in cosmetic emulsions. *Carbohydrate Polymers*, *93*, 644–650.

Gilbert, L., Picard, C., Savary, G., & Grisel, M. (2013). Rheological and textural characterization of cosmetic emulsions containing natural and synthetic polymers: Relationships between both data. *Colloids and Surfaces A—Physicochemical and Engineering Aspects*, *421*, 150–163.

Kim, C. A., Choi, H. J., Kim, C. B., & Jhon, M. S. (1998). Drag reduction characteristics of polysaccharide xanthan gum. *Macromolecular Rapid Communications*, *19*, 419–422.

Kim, C. A., Choi, H. J., Sung, J. H., Lee, H. M., & Jhon, M. S. (2005). Effect of solubility parameter of polymer-solvent pair on turbulent drag reduction. *Macromolecular Symposia*, *222*, 169–174.

Kim, C. A., Jo, D. S., Choi, H. J., Kim, C. B., & Jhon, M. S. (2001). A high-precision rotating disk apparatus for drag reduction characterization. *Polymer Testing*, *20*, 43–48.

Kim, C. A., Lim, S. T., Choi, H. J., Sohn, J. I., & Jhon, M. S. (2002). Characterization of drag reducing guar gum in a rotating disk flow. *Journal of Applied Polymer Science*, *83*, 2938–2944.

Lee, H. C., & Brant, D. A. (2002). Rheology of concentrated isotropic and anisotropic xanthan solutions. 1. A rodlike low molecular weight sample. *Macromolecules*, *35*, 2212–2222.

Liberatore, M. W., Pollauf, E. J., & McHugh, A. J. (2003). Shear-induced structure formation in solutions of drag reducing polymers. *Journal of Non-Newtonian Fluid Mechanics*, *113*, 193–208.

Lim, S. T., Choi, H. J., & Chan, C. K. (2005). Effect of turbulent flow on coil-globule transition of lambda-DNA. *Macromolecular Rapid Communications*, *26*, 1237–1240.

Lim, S. T., Hong, C. H., Choi, H. J., Lai, P. Y., & Chan, C. K. (2007). Polymer turbulent drag reduction near the theta point. *European Physics Letters*, *80*. Art No. 58003.

Malkin, A. Y., Nesyn, G. V., Ilyusnikov, A. V., & Manzhai, V. N. (2001). A method for monitoring polymer reactions in very dilute solutions. *Journal of Non-Newtonian Fluid Mechanics*, *97*, 195–206.

Mohsenipour, A. A., & Pal, R. (2013). The role of surfactants in mechanical degradation of drag-reducing polymers. *Industrial & Engineering Chemistry Research*, *52*, 1291–1302.

Morris, E. R. (1977). Molecular origin of xanthan solution properties. *Extracellular microbial polysaccharides. ACS symposium series* (vol 45) Washington, DC, USA: American Chemicl Society.

Muller, G., Anrhourrache, M., Lecourtier, J., & Chauveteau, G. (1986). Salt dependence of the conformation of a single-stranded xanthan. *International Journal of Biological Macromolecules*, *8*, 167–172.

Norton, I. T., Goodall, D. M., Frangon, S. A., Morris, E. R., & Ress, D. A. (1984). Mechanism and dynamics of conformational ordering in xanthan polysaccharide. *Journal of Molecular Biology*, *175*, 371–394.

Pereira, A. S., Andrade, R. M., & Soares, E. J. (2013). Drag reduction induced by flexible and rigid molecules in a turbulent flow into a rotating cylindrical double gap device: Comparison between poly(ethylene oxide), polyacrylamide, and xanthan gum. *Journal of Non-Newtonian Fluid Mechanics*, *202*, 72–87.

Renou, F., Petibon, O., Malhiac, C., & Grisel, M. (2013). Effect of xanthan structure on its interaction with locust bean gum: Toward prediction of rheological properties. *Food Hydrocolloids*, *32*, 331–340.

Rinaudo, M., Milas, M., & Lambert, F. (1983). H and C NMR investigation of xanthan gum. *Macromolecules*, *16*, 816–819.

Shetty, A. M., & Solomon, M. J. (2009). Aggregation in dilute solutions of high molar mass poly(ethylene) oxide and its effect on polymer turbulent drag reduction. *Polymer*, *50*, 261–270.

Sohn, J. I., Kim, C. A., Choi, H. J., & Jhon, M. S. (2001). Drag-reduction effectiveness of xanthan gum in a rotating disk apparatus. *Carbohydrate Polymers*, *45*, 61–68.

Sung, J. H., Kim, C. A., Choi, H. J., Hur, B. K., Kim, J. G., & Jhon, M. S. (2004). Turbulent drag reduction efficiency and mechanical degradation of poly(acrylamide). *Journal of Macromolecular Science B: Physics*, *43*, 507–518.

Suksamranchit, S., Sirivat, A., & Jamieson, A. M. (2006). Polymer-surfactant complex formation and its effect on turbulent wall shear stress. *Journal of Colloid and Interface Science*, *294*, 212–221.

Tam, K. C., & Tiu, C. (1993). Rheology of water-soluble polymers—A comparative-study on the effect of monovalent salt. *Polymer-Plastics Technology and Engineering*, *32*, 123–138.

Tiu, C., Moussa, T., & Carreau, P. J. (1995). Steady and dynamic shear properties of non-aqueous drag-reducing polymer solutions. *Rheologica Acta*, *34*, 586–600.

Wyatt, N. B., & Liberatore, M. W. (2010). The effect of counterion size and valency on the increase in viscosity in polyelectrolyte solutions. *Soft Matter*, *6*, 3346–3352.

Wyatt, N. B., Gunther, C. M., & Liberatore, M. W. (2011). Drag reduction effectiveness of dilute and entangled xanthan in turbulent pipe flow. *Journal of Non-Newtonian Fluid Mechanics*, *113*, 193–208.